Langmuir **1996,** *12,* 4987–4997

Acoustic Spectroscopy for Concentrated Polydisperse Colloids with High Density Contrast

Andrei S. Dukhin* and Philip J. Goetz

Pen Kem, Inc., 341 Adams Street, Bedford Hills, New York 10507

Received November 29, 1995. In Final Form: May 15, 1996[⊗]

The acoustic attenuation spectra for rutile dispersions show a pronounced nonlinear increase in attenuation over a volume fraction range from 1% to 42%. A theory is developed to explain this nonlinear effect. This theory takes into account hydrodynamic particle–particle interactions caused by a sound wave. The modification of the acoustic theory has been accomplished using a "cell model" and a "coupled phase theory". The notion of a "cell" allows us to take into account the hydrodynamic interaction between particles when calculating a drag coefficient. Furthermore, the mass conservation law helps to expand this "cell" concept to include the effects of polydispersity, introducing only one more adjustable parameter. This parameter determines the relationship between the cell and the particle radii. The "coupled phase theory", generalized here for a polydisperse structured system, relates this drag coefficient to both the attenuation and sound speed spectra. Experimental verification of the modified theory is presented. The rutile samples were well dispersed. The measured attenuation agrees quite well with the attenuation predicted by the new theory for the volume fraction up to 30%. However, in the most highly concentrated slurries it was necessary to postulate some degree of aggregation in order to reconcile the measured and predicted spectra. The modified theory provides a means to calculate reasonable bimodal particle size distributions in these cases.

Introduction

Loss Mechanisms. There are six known loss mechanisms for the interaction of sound with a dispersed system: (1) viscous; (2) thermal; (3) scattering; (4) intrinsic; (5) structural; and (6) electrokinetic.

The viscous losses of the acoustic energy occur due to the shear wave generated by the particle oscillating in the acoustic pressure field. These shear waves appear because of the difference in the densities of the particles and the medium. This density contrast causes the particle motion with respect to the medium. As a result the liquid layers in the particle vicinity slide relative to each other. This sliding nonstationary motion of the liquid near the particle is referred to as "shear wave".

The reason for the thermal losses is the temperature gradients generated near the particle surface. These temperature gradients appear due to the thermodynamic coupling between pressure and temperature.

The mechanism of the scattering losses is quite different compared to those of the viscous and thermal losses. Acoustic scattering does not produce the dissipation of the acoustic energy. It is similar to the light scattering. Particles simply redirect the part of the acoustic energy flow. As a result the portion of the sound energy does not reach the sound transducer.

The intrinsic losses of the acoustic energy occur due to the interaction of the sound wave with the materials of the particles and medium as homogeneous phases.

The oscillation of the network of the interparticle links in the structured dispersed system causes structural losses. Thus, this mechanism is specific for the structured systems.

Oscillation of the charge particles in the acoustic field leads to the generation of the alternating electrical field and, consequently, alternating electric current. As a result a part of the acoustic energy transforms to electric energy and then irreversibly to heat.

Only the first four mechanisms (viscous, thermal, scattering, and intrinsic) make a significant contribution to the overall attenuation spectra in most cases.[1] Structural losses are significant only in structured systems which require a quite different theoretical framework. For the present, there is no theory for describing these structural losses. Finally, the contribution of electrokinetic losses to the total sound attenuation is almost always negligibly small[2] and will be neglected.

Existing Theory and Limitations. The theory for these four most important mechanisms (viscous, thermal, scattering, and intrinsic) has already been developed by Epstein and Carhart,[3] as well as Allegra and Hawley,[1] *but only for the "monodisperse spherical dilute case"*. We will refer to this special case theory as the ECAH theory.

The term "monodisperse" is normally used to suggest that all of the particles are assumed to have the same diameter. Extensions of the ECAH theory to include polydispersity have typically assumed a simple linear superposition of the attenuation for each size fraction. In the present analysis we don't use the superposition assumption. At the same time we provide a framework for including not only polydispersity in the particle size but also polydispersity in other physical properties such as density. This provides the necessary framework to handle practical systems, e.g. mixtures of alumina and zirconia in a ceramic slurry.

The term "spherical" is used to denote that all calculations are performed assuming that each particle can be adequately represented as a sphere. We use the same model for the particles.

Most importantly, the term "dilute" is used to admit that there is no consideration of particle–particle interactions. This fundamental limitation normally restricts the application of the resultant theory to dispersions with a volume fraction of less than a few volume percent. However, there is some evidence that the ECAH theory, in *some very specific situations*, does nevertheless provide

[⊗] Abstract published in *Advance ACS Abstracts,* September 15, 1996.

(1) Allegra, J. R.; Hawley, S. A. Attenuation of Sound in Suspensions and Emulsions: Theory and Experiments. *J. Acoust. Soc. Am.* **1972,** *51,* 1545–1564.

(2) Strout, T. A. Attenuation of Sound in High-Concentration Suspensions: Development and Application of an Oscillatory Cell Model. Thesis, The University of Maine, 1991.

(3) Epstein, P. S.; Carhart, R. R. The Absorption of Sound in Suspensions and Emulsions. *J. Acoust. Soc. Am.* **1953,** *25* (3), 553–565.

S0743-7463(95)01085-7 CCC: $12.00

a correct interpretation of experimental data, even for volume fractions as large as 30%.

An early demonstration of the ability of the dilute ECAH theory to describe some concentrates was in fact provided by Allegra and Hawley. They observed almost perfect correlation between experiment and dilute case ECAH theory for several systems: a 20 vol % toluene emulsion; a 10 vol % hexadecane emulsion; and a 10 vol % polystyrene latex. Similar work with emulsions by McClements[4] has provided similar results. The recent work by Holmes, Challis, and Wedlock[23] shows the good agreement between ECAH theory and experiment even for 30 vol % polystyrene latices. However, it is important to note that the surprising validity of the dilute ECAH theory for moderately concentrated systems has only been demonstrated in systems where the "thermal losses" were dominant. We shall return to this point in a future paper (following paper in this issue).

Despite the limited success of the ECAH theory with emulsions and latices, the validity of the ECAH theory for moderately concentrated systems is still very much in doubt for systems in which, by contrast, the "viscous losses" are dominant. McClements[4,5] states that it is quite clear that particle–particle interactions must be included in any theory which purports to address concentrated industrial systems. An appropriate modified theory can then provide a unique basis for particle characterization at high volume fractions, where no other technique is so far available.

Hydrodynamic and Thermodynamic Fields. To set the stage, it should first be noted that particles interact with each other through both "hydrodynamic" and "thermodynamic" fields. The particles generate these fields in their immediate vicinity in response to the sound wave as it propagates through the dispersed system. Fortunately, it is possible to consider these hydrodynamic and thermodynamic interactions quite separately, which greatly simplifies the theoretical discussion.

In essence, the hydrodynamic field is responsible for the viscous loss whereas the thermodynamic field provides the thermal loss. In many cases, one mechanism is negligibly weak compared to the other. For instance, viscous losses are typically dominant for dispersions with a high density contrast ($\Delta\rho/\rho > 1$), such as oxides and pigments. On the other hand, thermal losses predominate in systems with a low density contrast and perhaps flexible particles, such as emulsions and latices. A "critical frequency" for a particular loss mechanism is typically defined as that frequency where the loss is greatest. It is important to note that the critical frequencies for the viscous and thermal losses are often quite remote from one another, a factor which permits us to consider theses effects separately, since one loss mechanism then reaches a maximum at a frequency where the other loss is negligibly weak.

This paper will deal only with the hydrodynamic particle–particle interaction, and for this discussion we will neglect particle–particle interactions as they relate to the thermodynamic fields. As a result this paper is targeted primarily at medium and high density contrast systems where the viscous losses are dominant and the thermal losses play only a supporting role. The question of the particle–particle interactions with respect to the thermodynamic fields will be addressed in a subsequent paper (following paper in this issue), which will address emulsions and latex materials.

It should be noted that the term "viscous loss" is something of a misnomer, since, in fact, it relates not only to pure "viscous" effects but also to "inertial" effects resulting from particle motion with respect to the liquid. The viscous component is dominant at lower frequencies, whereas a dissipative term associated with inertia becomes dominant at high frequencies.[6,7] This "inertial" term relates to the unsteady generation of vorticity in the boundary layer near the particle and its diffusion away from the particle surface.

Critical Frequency. According to the dilute ECAH theory, the critical frequency ω_{cr} is independent of the volume fraction. By definition, the critical frequency is that frequency for which the attenuation coefficient, expressed in dB/cm·MHz, reaches a maximum. Such a dilute system can be characterized by two key dimensions: the radius of the particle and the "viscous depth". The viscous depth is simply a measure of how deeply a shear wave can penetrate into the medium. The critical frequency is that frequency at which the viscous depth becomes comparable to the particle size. As a result, the critical frequency for the dilute system is inversely proportional to the square of the particle radius but is independent of concentration. We can thus express the critical frequency as

$$\omega_{cr} = \frac{9\nu\rho_0}{2a^2\rho_p} \tag{1.1}$$

where ν is a kinematic viscosity, ρ_0 and ρ_p are the densities of the medium and particle, respectively, and a is the particle radius.

The first goal in this paper is to show experimentally that, contrary to the dilute ECAH theory, the critical frequency for the viscous term is a nonlinear function of volume fraction. Whereas the particle size and the viscous depth are the only pertinent dimensions in a dilute system, an important new dimension is added in a concentrate, namely the gap between the particles. This gap becomes even smaller than the particle radius itself at high solid loading. In such concentrated cases, there is no longer room for the shear wave to penetrate into the medium on a scale comparable to the particle radius. We can say that the gap between the particles restricts the viscous depth as a result *the critical frequency becomes dependent on both the gap width and the particle radius*. As a result the critical frequency becomes a function of the volume fraction.

The second goal in this paper is to create a theory which explains this shift of the critical frequency to higher frequency with increases in volume fraction and to confirm this theory experimentally.

Long-Wavelength Requirement. We would like to keep the theory as general as possible. Nevertheless, one important simplification of the theory will be employed, the so-called "long-wave requirement",[1,2] which requires the wavelength of the sound wave λ to be much larger than the particle radius. Usually the condition $\lambda > 3a$ is used. This "long-wave requirement" restricts the sound frequency to be above some certain critical frequency ω_{lw}

(4) McClements, J. D. Ultrasonic Determination of Depletion Flocculation in Oil-in-Water Emulsions Containing a Non-Ionic Surfactant. *Colloids Surf.* **1994**, *90*, 25–35.

(6) Atkinson, C. M.; Kytomaa, H. K. Acoustic Wave Speed and Attenuation in Suspensions. *Int. J. Multiphase Flow* **1992**, *18*, 4, 577–592.

(7) Temkin, S.; Dobbins, R. A. Attenuation and Dispersion of Sound by Particulate-Relaxation Processes. *J. Acoust. Soc. Am.* **1966**, *40*, 317–

which is reciprocally proportional to the particle size according to the equation

$$\omega_{lw} = \frac{2\pi V_0}{3a} \tag{1.2}$$

where V_0 is the sound speed in the medium.

Comparing ω_{cr} with ω_{lw}, we can conclude that $\omega_{cr} \ll \omega_{lw}$ for the particles with size greater than 10 nm. It means that attenuation associated with the viscous losses is significant for the frequencies much lower than ω_{lw} when the particle size is more than 10 nm. Therefore, the long-wave requirement is valid for the theory of the viscous losses in the aqueous dispersions when the particle size is greater than 10 nm.

Invoking this long-wave requirement also permits us to simplify the analysis by considering viscous losses independently of scattering losses. Scattering losses are normally negligibly small compared to the viscous losses when the long-wave restriction on the sound frequency is valid, as illustrated in Appendix A.

Cell Model Approach. There are two approaches to the description of a nonequilibrium phenomenon such as sound propagation in a concentrated dispersed system. The first approach is the statistical mechanics of the liquid state. The statistical approach is widely used to study particle–particle interactions in the light scattering and rheological measurements.[8]

The second approach explores the idea of the "cell model".[9-11] There are several reasons to prefer the cell model approach for extending the theory of acoustic spectroscopy. For one, the cell model approach has already been successfully applied to various other hydrodynamic phenomena. For another, it is relatively simple to use. But most importantly, the cell model approach gives us the opportunity to introduce the important notion of polydispersity to the system. This unique ability to accommodate polydispersity, in our judgment, more than compensates for any lack of precision inherent in the cell model approach to the problem.

The cell model approach is based on the idea of a "scale hierarchy".[11] Most commonly, there are three scales employed in describing a colloid system: "microscopic"; "cell"; and "macroscopic".

The "microscopic" scale is obviously the smallest. At this scale we introduce the intensive parameters and the kinetic coefficients of the dispersion medium. The properties of the microscopically small elements of the medium such as viscosity, density, temperature, pressure, the chemical potentials of the dissolved components, etc. are the general characteristics of the dispersion phase. The dispersed phase is characterized in the same way, by the same set of intensive "microscopic" parameters.

The "cell scale" is the midrange scale. The sizes of the particulates determine the characteristic scale factor at this level. A conventional spherical envelope of liquid surrounding each particle can be considered a "cell". The condition that the volume fraction inside each cell is the same as the total volume fraction of solid φ defines the amount of liquid associated with the particle. The "cell model" has been used to date only for the monodisperse case, and as we will see, this will be extended to cover polydispersity.

The "macroscopic scale" is the largest. The whole system as an entity is the subject for characterization on this scale. In the case of a concentrated system, the experiment can normally be performed only at the macroscopic level because the observation of single particles usually requires dilution.

In this paper we speak of a cell hierarchy consisting of only three levels. A structured system might require an additional scale appropriately chosen to reflect this structure. This added scale would fall somewhere between the cell and macroscopic scales but is not discussed further here and will be the subject of a future paper. At the same time we will make the first step in describing the "structural losses" including the effect of the specific forces acting between particles. We assume that these forces create a network of links between particles. However, the particles retain their random space distribution. The last assumption releases us from the necessity to use the additional level of the cell hierarchy.

Acoustic spectroscopy involves all three levels of this cell hierarchy in the characterization procedure.

Most "a priori information" about the system comes at the microscopic scale. Such known microscopic properties might include the viscosity, density, and sound speed velocity of both the medium and particle.

Our desired information, in the form of some description of the particle size or other properties, is at the cell level.

The experimental data, i.e. the sound attenuation α and sound speed V, are derived on the macroscopic scale.

It is therefore necessary to formulate a link between the macroscopic and cell scales in order to calculate a particle size distribution (PSD) from the acoustic spectra. The acoustic spectroscopy theory should give us this link. Unfortunately, it provides this link for some assumed model system rather than a real natural system.

Model Assumptions. The replacement of the real system with a convenient model can potentially cause significant errors. It is possible that the model error predominates over all other errors, including experimental errors and errors inherent to the approximate mathematical calculations. Clearly, the model system should reflect the properties of the real system as completely as possible. However, it is sometimes impossible to achieve this goal in a given model system. This means that there are usually some restrictions on the applicability of a given model system. So let us speak now of possible model systems for both the media and the dispersed phase.

An "incompressible Newtonian liquid" is a common model for the dispersion medium and will be employed here. Similarly, a "spherical particle" is a common model for the dispersed phase particles, and this choice is suitable for many well dispersed stable systems.

Inclusion of the structural network of the colloid particles is an additional important requirement to the model because colloid structure contributes to the acoustic energy losses.

An appropriate "coupled phase" acoustic theory incorporating only "viscous losses" has been created for the monodisperse concentrated system by Gibson and Toksoz.[12] It is generalized in this paper for systems which are polydisperse in terms of particle size, density, sound speed, and internal structure.

(8) Chen, M.; Russel, W. B. Characteristics of Flocculated Silica Dispersions. *J. Colloid Interface Sci.* **1991**, *141* (2), 564–577.

(9) Happel, J. Viscous Flow in Multiparticle Systems: Slow Motion of Fluids Relative to Beds of Spherical Particles. *AICHE J.* **1958**, *4*, 197–201.

(10) Kuvabara, S. The Forces Experienced by Randomly Distributed Parallel Circular Cylinders or Spheres in a Viscous Flow at Small Reynolds Numbers. *J. Phys. Soc. Jpn.* **1959**, *14*, 527–532.

(11) Shilov, V. N.; Zharkih, N. I.; Borkovskaya, Yu. B. Theory of Nonequilibrium Electrosurface Phenomena in Concentrated Disperse System. 1. Application of Nonequilibrium Thermodynamics to Cell Model. *Colloid J.* **1981**, *43* (3), 434–438.

(12) Gibson, R. L.; Toksoz, M. N. Viscous Attenuation of Acoustic Waves in Suspensions. *J. Acoust. Soc. Am.* **1989**, *85*, 1925–1934.

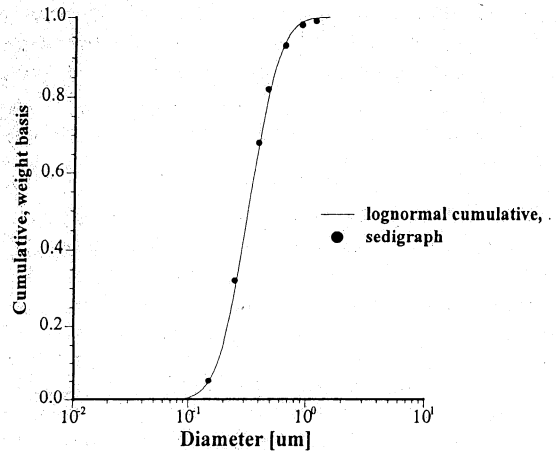

Figure 1. Cumulative particle size distribution on the weight basis of the rutile R746 measured with Sedigraph and approximated using the log–normal assumption. The median size of the log–normal distribution is 0.33 μm, and the standard deviation is 0.2.

The main characteristic of the fractional viscous losses is a drag coefficient Ω of the particles of a given fraction. The traditional nonstationary "cell model" is generalized for the polydisperse system to calculate the drag coefficient. The cell boundary conditions are used in the Happel's version.[9] The first successful attempt to apply the "cell model" for calculation of the nonstationary drag coefficient was performed in ref 2.

The experimental confirmation of the expanded theory is the third goal of this paper. It will be shown that the expanded theory is able to explain the nonlinear volume fraction effect in concentrated rutile dispersions and provide a reasonable particle size distribution.

Dilution Experiment with Concentrated Rutile Dispersion

Experimental Materials and Methods. The starting material was a concentrated aqueous rutile slurry obtained from E. I. DuPont de Nemours. It is commercially referred to as R746 and is normally supplied at a weight fraction of 76.5% (44.5% by volume). The density of the particles is 4.06 g/cu·cm. It is slightly less than that for the regular rutile because of the various surface modificators used to stabilize the slurry. The sample was then diluted to 0.83%, 2.92%, 4.95%, 9.81%, 17.47%, 24.71%, and 34.92% by volume using distilled water, adjusted to pH 8.5 with potassium hydroxide.

The particle size distribution (PSD) has been measured by Dr. Beloga from E. I. DuPont using Sedigraph 5100. This measurement has been performed for the very dilute system with and without sonication. The sonication effect turns out to be insignificant. The cumulative PSD is shown in Figure 1.The measured cumulative curves are not completed because Sedigraph is not able to characterize a PSD below 0.2 μm. Interpretation of the acoustic experiment requires the entire particle size distribution. Fortunately a log–normal distribution with the median size 0.33 μm and standard deviation 0.2 gives perfect extrapolation of the Sedigraph measured PSD. Figure 1 illustrates this fact. Thus, we will use the above-mentioned log–normal distribution as the PSD of the well dispersed stable dilute rutile dispersion R746.

The attenuation spectra were measured for the original concentrate and each of the seven diluted samples using the Pen Kem AcoustoPhor 8000. The attenuation was measured over a frequency range from 1 to 100 MHz. Each measurement was made three times and then repeated three times more after 24 h. The good reproducibility showed by this test indicated the

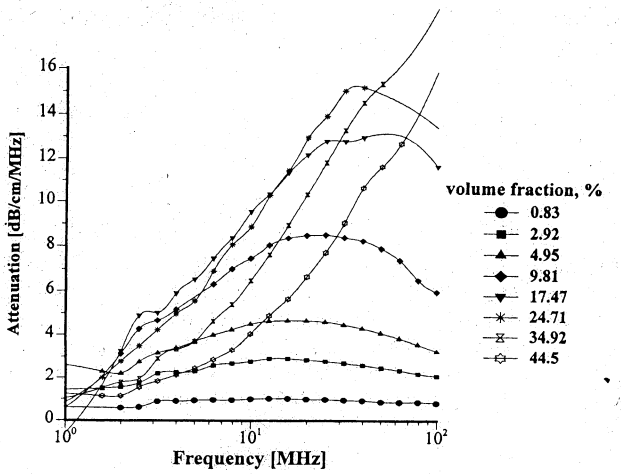

Figure 2. Attenuation spectra for the rutile dispersions (DuPont R746) with various volume fractions from 0.83 vol % to 44.5 vol %.

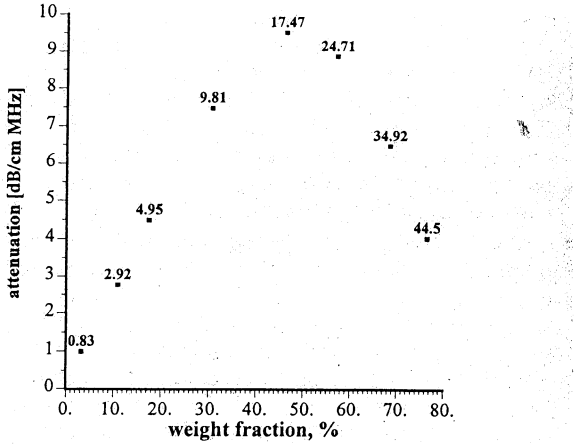

Figure 3. Dependence of the attenuation at the frequency 15 MHz on the dispersed system weight fraction. Corresponding volume fractions in percent are shown as the data point labels.

Some experimental points at low frequency (<2 MHz) and at high frequency (>50 MHz when φ > 10%) are excluded because of the large errors. (Those frequencies lie in the too close vicinities of the transducer piezocrystal harmonics.)

The set of the attenuation spectra corresponding to a volume fraction up to 25% shows that the critical frequency definitely shifts to the higher frequencies. This confirms the qualitative conclusion made earlier about the nonlinear volume fraction effect.

The attenuation dependence on volume fraction is shown in Figure 3 at a single frequency of 15 MHz. It is seen that the dependence is extremely nonlinear above a volume fraction of 10%.

It is important to mention that ECAH theory is not able to explain the observed peculiarities of the attenuation spectra. If we assume that this theory retains its validity at the higher volume fractions, we must conclude that the increase of the solid concentration somehow leads to the destroying of the initial 0.33 μm singlets and the creation of smaller particles. This possibility seems quite unlikely.

The result of this experiment seems sufficient justification for attempting to create an expanded theory for concentrates.

Coupled Phase Theory for the Polydisperse Structured System

The basis of the coupled phase theory [12] is the balance

the unknown "effective" pressure P^* and the velocities of the particles $\boldsymbol{u}_p$ and the media $\boldsymbol{u}_0$:

$$-\varphi\nabla P^* = \varphi\varrho_p\frac{\partial u_p}{\partial t} + \gamma(u_p - u_0) \quad (2.1)$$

$$-(1-\varphi)\nabla P^* = (1-\varphi)\varrho_0\frac{\partial u_0}{\partial t} - \gamma(u_p - u_0) \quad (2.2)$$

$$-\frac{\partial P^*}{\partial t} = K^*(1-\varphi)\nabla u_0 + K^*\varphi\nabla u_p \quad (2.3)$$

where

$$\gamma = \frac{9\eta\varphi\Omega}{2a^2} \quad (2.4)$$

K^* is a stress modulus (the reciprocal of compressibility) of the disperse system, t is time, and η is the dynamic viscosity of the medium.

The time and space dependence of the unknown field variables P^*, u_o, and u_p is presented as a monochromatic wave $Ae^{j(\omega t - lx)}$, where j is a complex unit and l is a complex wavenumber. The attenuation coefficient and sound speed are related to the complex wavenumber by the following expressions:

$$\alpha = -\mathrm{Im}(l) \quad (2.5)$$

$$V = \omega/\mathrm{Re}(l) \quad (2.6)$$

Substitution of the field variables as monochromatic waves into the system of eqs 2.1−2.3 yields a system of three algebraic equations for the monochromatic amplitudes A. This system has a nontrivial solution if the main determinant equals zero, in which case one can calculate the value of the complex wavenumber. The following expression for **l** has been derived in ref 12:

$$\frac{l^2K^*}{\omega^2\varrho^*} = \frac{\varphi(1-\varphi)\dfrac{\varrho_0\varrho_p}{\varrho^*} - j\dfrac{\gamma}{\omega}}{\varphi(1-\varphi)\varrho^* - j\dfrac{\gamma}{\omega}} \quad (2.7)$$

where

$$\varrho^* = \varrho_p\varphi + \varrho_0(1-\varphi) \quad (2.8)$$

$$\varrho' = \varrho_0\varphi + \varrho_p(1-\varphi) \quad (2.9)$$

Expression 2.7 reflects only the influence of the viscous loss mechanism on the propagation of the sound through a monodisperse system. As a result, the coupled phase theory created in the work[12] is valid only for monodisperse particles in nonstructured systems.

It is possible to generalize this "coupled phase" theory for a structured polydisperse system. The same idea of the forces balance can be applied for the particles in each size fraction of the polydisperse system independently. The number of fractions N is conventional and unlimited. The analog of the monodisperse system of eqs 2.1−2.3 contains $N+2$ equations for the polydisperse case. There are N equations for particles, 1 equation for the dispersion medium, and 1 more for the disperse system as a whole.

Structural Effects. Each balance forces equation should be modified because the "specific" forces[13,14] must be taken into account as well as the hydrodynamic ones. Specific forces act like springs connecting particles following the general transient-network theory created in refs 15 and 16. The simplified version of this model allows one to calculate the complex wave number.

Two terms are necessary to present adequately the contribution of the non-Hookean springs to the force balance. The first term is a Hook's force proportional to the displacement of the particle with the coefficient β_i. The second term is a dissipative force proportional to the particle velocity with the coefficient δ_i. The coefficients β_i and δ_i are assumed to be the same for all particles of the given ith fraction. This assumption is valid for a regular structure when the environment of the particles depends only on its size but not on its location. This assumption is a logical first step in incorporating structural effects in the theory of sound propagation through a polydisperse system.

The modified system of the $N+2$ balance equations can be presented as follows:

$$-\varphi_i\nabla P^* = \varphi_i\varrho_p^i\frac{\partial^2 x_p^i}{\partial t^2} + \gamma_i\left(\frac{\partial x_p^i}{\partial t} - u_0\right) + \beta_i x_p^i + \delta_i\frac{\partial x_p^i}{\partial t} \quad (2.10)$$

$$-(1-\varphi)\nabla P^* = (1-\varphi)\varrho_0\frac{\partial u_0}{\partial t} - \sum_{i=1}^{N}\gamma_i\left(\frac{\partial x_p^i}{\partial t} - u_0\right) \quad (2.11)$$

$$-\frac{\partial P^*}{\partial t} = K^*(1-\varphi)\nabla u_0 + \sum_{i=1}^{N}K^*\varphi_i\nabla\frac{\partial x_p^i}{\partial t} \quad (2.12)$$

where eq 2.10 is equivalent to N equations because i varies from 1 to N.

There are $N+2$ unknown field variables in the system (eqs 2.10−2.12): P^*, u_o, and x_p^i. The presentation of the field variables in the monochromatic wave form allows one to exclude time and space derivatives. The system of the equations for the unknown amplitudes is

$$\varphi_i jlP^* = -\varphi_i\varrho_p^i\omega^2 x_p^i + \gamma_i j\omega x_p^i - \gamma_i u_0 + \beta_i x_p^i + \delta_i j\omega x_p^i \quad (2.13)$$

$$(1-\varphi)jlP^* = (1-\varphi)\varrho_0 j\omega u_0 - \sum_{i=1}^{N}\gamma_i(j\omega x_p^i - u_0) \quad (2.14)$$

$$j\omega P^* = K^*(1-\varphi)jlu_0 - \sum_{i=1}^{N}K^*\varphi_i\omega l x_p^i \quad (2.15)$$

where the symbols defining amplitude are the same as before in the system (eqs 2.10−2.12) for the corresponding field variables.

The same condition of the nontrivial solution existence leads to the equation for the complex wavenumber. This

(13) Derjaguin, B. V. Theory of Stability of Colloids and Thin Films. Consultants Bureau, New York, 1989.
(14) Overbeek, J. Th. G. Recent Developments in the Understanding of Colloid Stability. *J. Colloid Interface Sci.* **1977**, *58*, 408−422.
(15) Macosko, W. C. Rheology: Principles, Measurements and Applications; VCH: New York, 1992.
(16) Kamphuis, H.; Jongschaap, R. J. J.; Mijnlieff, P. F. A Transient-Network Model Describing the Rheological Behaviour of Concentrated Dispersions. *Rheol. Acta* **1984**, *23*, 329−344.

Table 1

$\varphi_1 jl$	γ_1	$\varphi_1\rho_p{}^1\omega^2 - j\omega\gamma_1 - \beta_1 - j\omega\delta_1$	0	0
i	i	i	i	i
$\varphi_N jl$	γ_N	0	i	$\varphi_N\rho_p{}^N\omega^2 - j\omega\gamma_N - \beta_N - j\omega\delta_N$
$jl(1-\varphi)$	$-\Sigma\gamma_i - (1-\varphi)j\omega\rho_0$	$j\omega\gamma_1$	$j\omega\gamma_i$	$j\omega\gamma_N$
$j\omega$	$-K^*(1-\varphi)jl$	$K^*\omega l\varphi_1$	$K^*\omega l\varphi_i$	$K^*\omega l\varphi_N$

condition requires the main determinant to be equal to zero:

$$\mathrm{Det}(l) = 0 \tag{2.16}$$

where Det is the determinant of the $N + 2$ order shown in Table 1.

The order of the determinant can be reduced to 2 using the method of mathematical induction and the standard procedure of lowering the determinant order.[17] As a result Det equals

$$\begin{matrix} (1-\varphi) + \sum_{i=1}^{N}\frac{j\omega}{D} & -j\omega\left[\varrho_0(1-\varphi) + \sum_{i=1}^{N}\frac{\gamma_i(\mathrm{Den}_i - j\omega\gamma_i)}{j\omega\ \mathrm{Den}_i}\right] \\ \frac{j\omega}{l^2K^*} + \sum_{i=1}^{N}\frac{j\omega\varphi_i}{\mathrm{Den}_i} & (1-\varphi) + \sum_{i=1}^{N}\frac{j\omega\varphi_i\gamma_i}{\mathrm{Den}_i} \end{matrix}$$

where

$$\mathrm{Den}_i = -\omega^2\varrho_p^i\varphi_i + j\omega\gamma_i + j\omega\delta_i + \beta_i$$

This simplification allows us to solve eq 2.16 with respect to the complex wavenumber l. The result is the following:

$$\frac{l^2K^*}{\omega^2} = \frac{(-\varphi)\varrho_0 + \sum_{i=1}^{N}\frac{\gamma_i(\mathrm{Den}_i - j\omega\gamma_i)}{j\omega\mathrm{Den}_i}}{\left[1-\varphi+\sum_{i=1}^{N}\frac{j\omega\varphi_i\gamma_i}{\mathrm{Den}_i}\right]^2 - \sum_{i=1}^{N}\frac{\omega^2\varphi_i^2}{\mathrm{Den}_i}\left[(1-\varphi)\varrho_0 + \sum_{i=1}^{N}\frac{\gamma_i(\mathrm{Den}_i - j\omega\gamma_i)}{j\omega\ \mathrm{Den}_i}\right]} \tag{2.17}$$

Advantages of the Extended Coupled Phase Theory. Expression 2.17 is much more general than the original "coupled phase theory". First of all, it is valid for the polydisperse system whereas expression 2.7 fits only the monodisperse case. This is very important, since practical systems might be polydisperse not only in size but also in density or other physical properties. The more general theory allows us to treat systems with mixed dispersed phases containing particles of different chemical nature and different internal structure.

The ability to handle agglomeration effects is the second advantage of the more general theory. It allows us to calculate α and V of a flocculated system when the structural scale is larger than the wavelength but is much shorter than the system dimensions. The effective volume fraction in this case φ_{eff} is higher than the volume fraction of solid φ because particles are being concentrated into the floccules by the specific forces. This effect of the particle concentration is the additional showing up of the structure.

The special "volume correction coefficient" σ

$$\sigma = \frac{\varphi_{eff}}{\varphi} \tag{2.18}$$

characterizes the relative importance of this effect. Acoustic energy dissipates predominantly inside the floccules whereas expression 2.17 gives the attenuation coefficient with respect to the total volume of the system.

Expression 2.17 becomes much simpler in the case of nonstructured systems. The coefficients β and δ equal zero in this case. Assuming also the same density for all particles, expression 2.17 can be transformed to

$$\frac{l^2K^*}{\omega^2\varrho^*} = \frac{1 - \frac{\varrho_p}{\varrho}\sum_{i=1}^{N}\frac{\varphi_i}{1 - \frac{9j\varrho_0}{4s_i^2\varrho_p}\Omega_i}}{1 + \left(\frac{\varrho^*}{\varrho_p} - 2\right)\sum_{i=1}^{N}\frac{\varphi_i}{1 - \frac{9j\varrho_0}{4s_i^2\varrho_p}\Omega_i}} \tag{2.19}$$

Application of this extended version of the "coupled phase theory" requires an expression for the drag coefficient of the particles in the concentrated polydisperse system. The concept of "cell model" allows us to solve this problem. The generalization of the "cell model" for the polydisperse system is the necessary first step.

Cell Model for Polydisperse System

The main idea of the "cell model" is that each particle in the concentrated system is considered separately inside a spherical cell of liquid associated only with a given individual particle. The cell boundary conditions formulated on the outer boundary of the cell reflect the particle–particle interaction.

In the past, the cell model has been applied only to monodisperse systems. This restriction allows one to define the radius of the cell. Equating the solid volume fraction of the each cell to the volume fraction of the entire system yields the following expression for the cell radius b

$$b = \frac{a}{\varphi^{1/3}} \tag{3.1}$$

In the case of a polydisperse system, the introduction of the cell is more complicated because the liquid can be distributed between fractions in an infinite number of ways. However, the condition of mass conservation is still necessary.

Each fraction can be characterized by particle radii a_i, cell radii b_i, the thickness of the liquid shell in the spherical cell $h_i = b_i - a_i$, and the volume fraction φ_i. The mass conservation law relates these parameters together as follows:

$$\sum_{i=1}^{N}\left(\frac{b_i}{b}\right)^3$$

Expression 3.2 might be considered as an equation with N unknown parameters h_i. An additional assumption is still necessary to determine the cell properties for the polydisperse system. This additional assumption should define the relationship between particle radii and shell thickness for each fraction. We suggest the following simple relationship:

$$h_i = h a_i^n \tag{3.3}$$

This assumption reduces the number of unknown parameters to only two which are related by the following expression:

$$\sum_{i=1}^{N} [1 + h a_i^{n-1}]^3 \varphi_i = 1 \tag{3.4}$$

It is convenient to calculate the values of h for the various values of n. The parameter n will be referred to as a "shell factor". Two specific values of the shell factor correspond to easily understood cases. A shell factor of 0 depicts the case in which the thickness of the liquid layer is independent of the particle size. A shell factor of 1 corresponds to the normal "superposition assumption", which gives the same relationship between particles and cell radii in the monodisperse case; i.e., each particle is surrounded by a liquid shell which provides each particle the same volume concentration as the volume concentration of the overall system. In general, the "shell factor" is considered an adjustable parameter because it adjusts the dissipation of energy within the cells.

Nonstationary Cell Model

The hydrodynamics of an incompressible liquid allows us to calculate the drag coefficient of the particle provided the "long-wave requirement" is valid. The drag coefficient Ω relates the hydrodynamic force exerted on the particle F_h to the particle velocity u_p:

$$F_h = 6\pi\eta a \omega u_p \tag{4.1}$$

The hydrodynamic field u and pressure field P around the particle moving with the velocity u_p are necessary to calculate the hydrodynamic F_h. Again noting that we assume the long-wave requirement is valid, the following traditional set of the hydrodynamic equations allows us to calculate these fields:

$$-\varrho_0 \frac{du}{dt} = \eta \text{ rot rot } u + \text{grad } P \tag{4.2}$$

$$\text{div } u = 0 \tag{4.3}$$

This system of equations requires the boundary conditions for both the radial u_r and tangential u_θ components of the liquid velocity at the surface of the particle,

$$u_r(r=a) = u_p \tag{4.4}$$

$$u_\theta(r=a) = -u_p \tag{4.5}$$

as well as the velocity components on the outer surface of the cell,

$$\Pi_{r\theta}(r=b) = \eta\left(\frac{1}{r}\frac{\partial u_r}{\partial \theta} + r\frac{\partial \frac{u_\theta}{r}}{\partial r}\right) = 0 \tag{4.6}$$

$$u_r(r=b) = 0 \tag{4.7}$$

The boundary condition on the cell surface (eq 4.6) corresponds to Happel's version of the cell model.[9,18]

The general solution of this nonstationary hydrodynamic problem is given by the following expressions:

$$u_r(r) = C\left(1 - \frac{b^3}{r^3}\right) + \frac{2}{3}\int_r^b \left(1 - \frac{x^3}{r^3}\right) h(x)\, dx \tag{4.8}$$

$$u_\theta(r) = -C\left(1 + \frac{b^3}{2r^3}\right) - \frac{2}{3}\int_r^b \left(1 + \frac{x^3}{2r^3}\right) h(x)\, dx \tag{4.9}$$

where

$$h(x) = C_1 h_1(x) + C_2 h_2(x) \tag{4.10}$$

$$h_1(x) = \frac{e^{-x(1+j)}}{x^2}(-x + j(1+x)) \tag{4.11}$$

$$h_2(x) = \frac{e^{x(1+j)}}{x^2}(x + j(1-x)) \tag{4.12}$$

The boundary conditions allow us to calculate three unknown constants C, C_1, and C_2:

$$C = -\frac{b}{3}C_1 h_1(b) - \frac{b}{3}C_2 h_2(b) \tag{4.13}$$

$$C_1 = \frac{h_2(b) - \frac{2I_{23}}{b}}{\text{Den}} \tag{4.14}$$

$$C_2 = -\frac{h_1(b) - \frac{2I_{13}}{b}}{\text{Den}} \tag{4.15}$$

where

$$\text{Den} = I_1\left(h_2(b) - \frac{2I_{23}}{b}\right) - I_2\left(h_1(b) - \frac{2I_{13}}{b}\right) + h_1(b)I_{23} - h_2(b)I_{13} \tag{4.16}$$

$$I_1 = -j\frac{e^{-x(1+j)}}{x}$$

$$I_2 = -j\frac{e^{x(1+j)}}{x}$$

$$I_{13} = -\frac{e^{-x(1+j)}}{b^3}(1.5(1+x) + j(x^2 + 1.5x))$$

$$I_{23} = -\frac{e^{x(1+j)}}{b^3}(1.5(-1+x) + j(-x^2 + 1.5x))$$

Expressions 4.8–4.16 determine the hydrodynamic field around the oscillating particle. The hydrodynamic force

(18) Happel, J.; Brenner, H. *Low Reynolds Number Hydrodynamics*; Martinus Nijhoff Publishers: Dordrecht, The Netherlands, 1973.
(19) Press, W. H.; Teukolsky, S. A.; Vetterling, W. T.; Flannery, B. P. *Numerical Recipes in C*, 2nd ed.; Cambridge University Press: New York, 1992.
(20) Phillips, D. L. A Technique for the Numerical Solution of Certain Integral Equations of the First Kind. *J. Assoc. Comput. Mach.* **1962**, *9* (1), 84–97.
(21) Twomey, S. On the Numerical Solution of Fredholm Integral Equation of the First Kind by the Inversion of the Linear System Produced by Quadrature. *J. Assoc. Comput. Mach.* **1963**, *10* (1), 97–101.

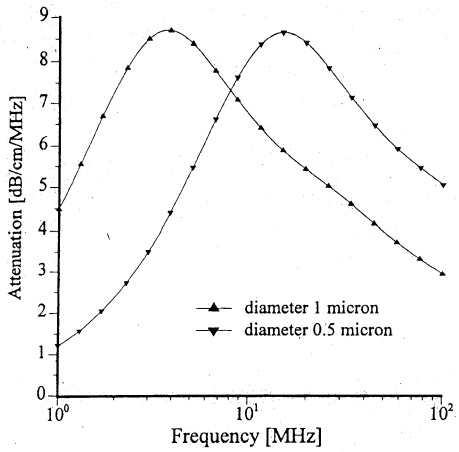

Figure 4. Attenuation spectra for two monodisperse systems with particle diameters 1 and 0.5 μm. The volume fraction is 20%.

exerted on the particle can then be calculated as a surface integral of the stress tensor:[18]

$$F_p = -\frac{2\pi a^3\sqrt{2\eta\rho\omega}}{3}\left[\left(-\frac{dh(r)}{dr}a + h(r)\right) + 2jsu_\theta\right]|_{r=a} \tag{4.17}$$

where

$$s = \frac{a\sqrt{\omega}}{\sqrt{2\nu}}$$

Substitution of eq 4.17 into eq 4.1 gives the following expression for the desired drag coefficient:

$$\Omega = \frac{s^2}{3}\left[C_1\left(-\frac{dh_1}{dr}a + \frac{h_1}{s}\right) + C_2\left(-\frac{dh_2}{dr}a + \frac{h_2}{s}\right) - \frac{4j}{3}\right] \tag{4.18}$$

This expression contains both dissipative terms: viscous and inertial.

Expression 4.18 allows us to calculate the fractional drag coefficients in the general equation for the complex wavenumber (eq 2.17). The radius of the cell b can be calculated according to the algorithm suggested in the previous section. Therefore, expression 4.18 makes this version of the theory of the viscous and structural losses complete.

Dependence of the Attenuation and Sound Speed Spectra on the Distribution of the Particle Size and Volume Fraction

The graphs presented in Figures 4–8 illustrate the dependencies of the attenuation on the various disperse system parameters. All spectra correspond to the non-structured system (i.e. $\beta = 0$; $\delta = 0$). All spectra reflect only the viscous loss contributions to the attenuation over the frequency range from 1 to 100 MHz. The pertinent properties of particles in all size fractions and of the media are shown in Table 2.

Attenuation is in dB/cm·Mhz in all figures.

Dependence on Mean Size for Monodisperse Sample. Figure 4 illustrates the dependence of the attenuation spectra on the particle diameter for a monodisperse system having a volume fraction of 20%.

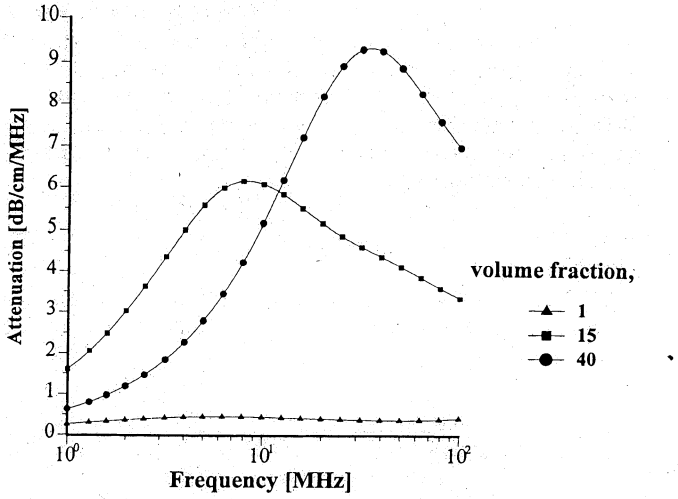

Figure 5. Attenuation spectra for two monodisperse systems with volume fractions 1%, 15%, and 40%. The particle diameter is 0.5 μm.

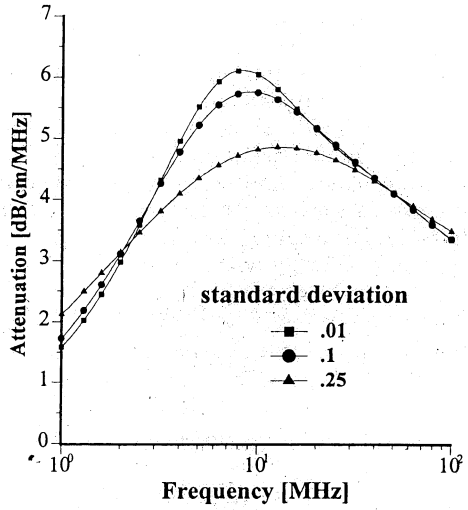

Figure 6. Attenuation spectra for polydisperse systems with different widths of the log–normal PSD. The standard deviations are 1%, 10%, and 25%. The particle diameter is 0.5 μm, and the volume fraction is 15%.

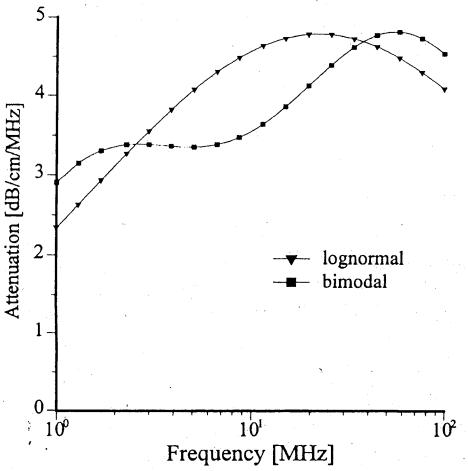

Figure 7. Attenuation spectra for polydisperse systems with log–normal and bimodal PSDs. The mean diameter is 0.5 μm, the standard deviation is 40%, and the volume fraction is 15% for both distributions. The ratio of the mode mean sizes for the bimodal distribution is 5.8.

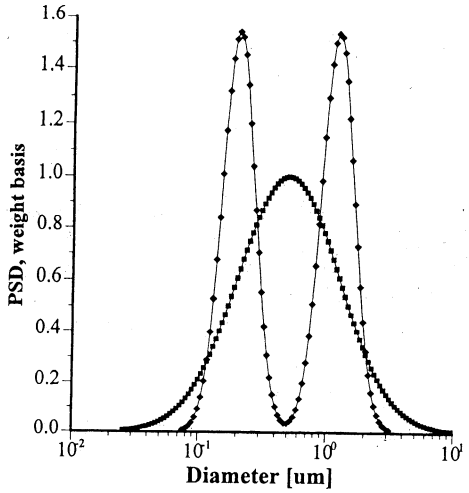

Figure 8. Log–normal and bimodal PSDs in the systems with diameter 0.5 μm and standard deviation 40%. The ratio of the mode mean sizes for the bimodal distribution is 5.8.

Table 2. Properties of the Sample Used in the Illustrative Figures 4–8

parameter	particle	media
density, g/cc	3	1
sound speed, m/s	6000	1500
dynamic viscosity, cP		1

frequency. For very large particles the critical frequency may be lower. As a result, at higher volume fractions the larger particles can be characterized with acoustic spectroscopy.

Dependence on Size Polydispersity. Figure 6 shows the dependencies of the attenuation spectra on the width of the particle size distribution for the system with the mean diameter 0.5 μm and the volume fraction 15%. The particle diameter distribution is log–normal. An increase of the standard deviation makes the attenuation spectra flatter and moves them to higher frequencies.

Dependence on Shape of the Particle Size Distribution. Figures 7 and 8 illustrate the dependence of the attenuation spectrum on the shape of the particle diameter distribution. The corresponding PSDs are presented in Figure 8. One is log–normal; the other one is bimodal. Each mode of the second one is a log–normal distribution. The mean diameter and total standard deviation are the same for both spectra. The mean size is 0.5 μm, the total standard deviation is 40%, and the volume fraction is 15%. The ratio of the mode sizes for the bimodal distribution is 5.8. The change in the shape of the distribution causes a significant change in the shape of the attenuation spectra. It is the illustration of the acoustic spectroscopy capability to characterize the aggregation phenomena.

Interpretation of the Dilution Experiment Performed with Rutile Dispersion

The sound attenuation measured for the rutile dispersion (Figure 2) is caused by viscous losses. Scattering losses are not significant because of the small particle size, as is shown in Appendix A. Thermal losses of the rutile are also negligibly small in the given frequency range from 1 to 100 MHz. Thus, the experimental attenuation presented in Figure 2 can be used as a test for the created theory. The given rutile dispersion is convenient for performing the theory test because all the input parameters required for viscous loss calculations are known. The set input parameters includes the particle size distribution, the density, and the sound speed of the dispersed phase and the dispersion medium weight fraction.

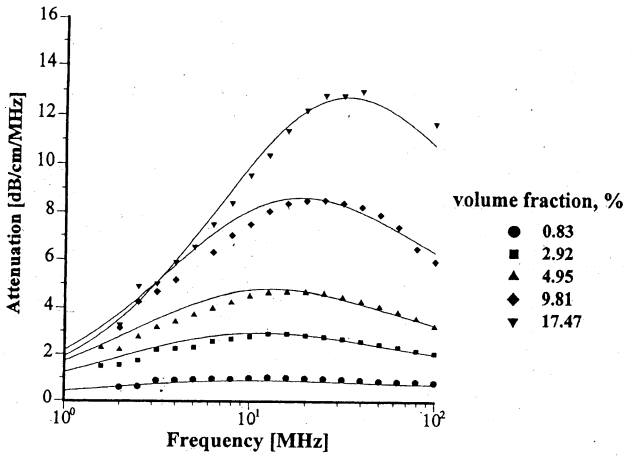

Figure 9. Experimental and theoretical attenuation spectra for the low and moderate volume fractions indicated in the legend. The PSD is the log–normal shown in Figure 1.

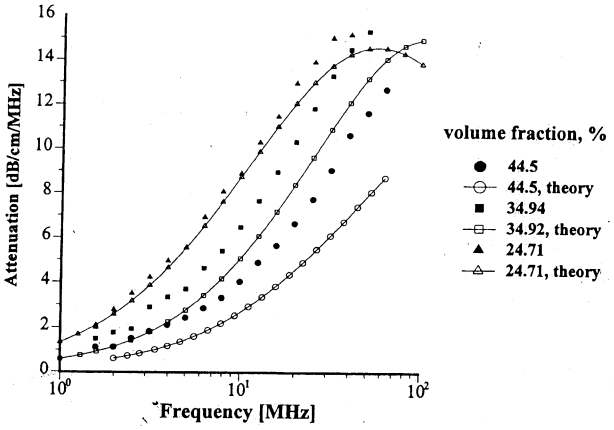

Figure 10. Experimental and theoretical attenuation spectra for the high volume fractions indicated in the legend. The PSD is the log–normal shown in Figure 1.

Figures 9 and 10 illustrate the relationship between calculated attenuation and experiment for the low and moderate volume fractions (Figure 9) and high volume fraction (Figure 10). It is seen that the correlation between theory and experiment is very good up to volume fraction 30%.

There are some deviations between calculated and measured attenuation for the two most concentrated samples with volume fraction above 30%. We think that these deviations reflect the change in the particle size distribution caused by the aggregation phenomena in the concentrated samples. The log–normal distribution measured with Sedigraph for the dilute system and shown in Figure 1 is not adequate for the high concentration samples. It is reasonable to assume that the particle builds aggregates, which leads to the change of the PSD. The particle size distribution becomes bimodal.

The bimodal hypothesis allows us to fit experimental attenuation curves, as is shown in Figure 11 for the most concentrated sample. The corresponding bimodal PSD is shown in Figure 12.

It is important to mention that the hypothesis of the bimodal PSD does not help ECAH theory. The assumption of aggregate formation shifts ECAH theory attenuation curves to lower frequencies whereas experiment shows a shift to higher frequencies. Thus, the hypothesis of a bimodal PSD works only in combination with hydrodynamic particle–particle interactions.

Conclusions

The dilution experiment performed with the rutile dispersion shows a strong nonlinear dependence of the

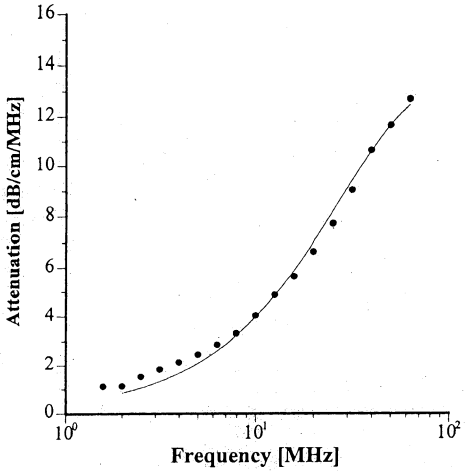

Figure 11. Experimental and theoretical attenuation spectra for the most concentrated sample with the volume fraction 44.5%. The bimodal PSD is shown in Figure 12.

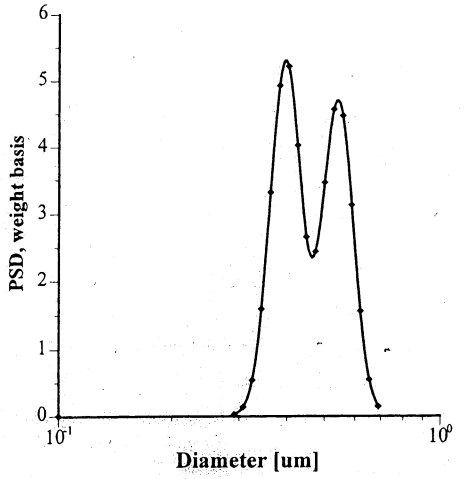

Figure 12. Bimodal particle size distribution providing the theoretical attenuation spectra shown in Figure 11 for the 44.5% volume fraction.

attenuation coefficient on the volume fraction. This experiment justifies the generalization of the theory describing sound propagation through the dispersed system.

The generalization of the "coupled phase theory" performed in this paper expands significantly the limits of the theoretical interpretation of the attenuation spectra including polydisperse systems. The "coupled phase theory" requires information about particle drag coefficients. The assumption about particle spherical shape allows us to use the "cell model" as a convenient approach to calculate drag coefficients. The generalization of the "cell model" to the polydisperse case requires at least one additional parameter. The mass conservation law helps to introduce this parameter, referred to as the "shell factor". This additional parameter adjusts the value of the energy dissipation in the cell. The shell factor should be the subject of the optimization procedure as well as other unknown characteristics of the system such as particle size distribution.

The new theory takes into account two mechanisms of sound attenuation: viscous and structural losses. This makes it valid for the concentrated system containing rigid dense submicron particles when the sound frequency lies between 1 and 100 MHz. The new general version of the theory makes it possible to calculate the particle size

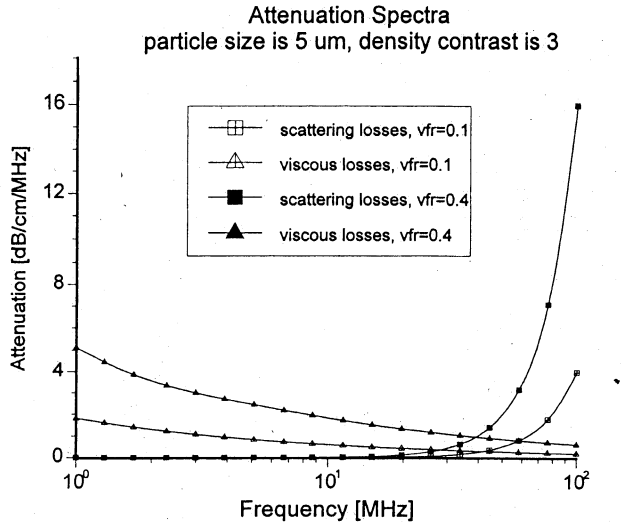

Figure 13. Attenuation spectra caused by the scattering and viscous losses for the two disperse sytems with volume fractions 10% and 40%. The particle size is 5 μm, the density contrast is 3, and the compressibility of the particle is much less than the compressibility of the liquid.

floccules, (d) a mixed polydisperse system containing two or more chemically different dispersed phases, and (e) a polydisperse system with macroscopic structure.

The new theory has been successfully tested. The particle size distribution measured independently with Sedigraph provides attenuation spectra matching experimentally measured attenuation spectra for volume fractions up to 30%.

Characterization of the dispersed system with acoustic spectroscopy makes it possible to characterize aggregation phenomena.

Acknowledgment. The authors would like to thank Dr. M. Baloga from E. I. DuPont for providing the rutile dispersion and Sedigraph data of the rutile particle size distribution.

Appendix A. Relative Contribution of the Viscous and Scattering Losses

A particle oscillating under the influence of sound also generates a compression wave. The part of the acoustic energy redistributed from the primary sound wave to the induced compression wave does not reach the receiver of the sound. This mechanism of the acoustic attenuation is referred to as "scattering losses". It is similar to some extent to light scattering.

The theory of scattering losses in concentrated disperse systems should take into account multiple scattering effects and hydrodynamic interactions between particles. However, it turned out that these two factors are not significant for suspensions of rigid solid particles.

The multiple scattering effect is small compared to the single scattering effect, according, for instance, to ref 22.

The relationship between viscous and scattering losses is illustrated in Figure 13 for dilute (φ = 10%) and concentrated systems (φ = 40%). The scattering attenu-

(22) Barrrett-Gultepe, M. A.; Gultepe, M. E.; McCarthy, J. L.; Yeager, E. B. A Study of Steric Stability of Coal–Water Dispersions by Ultrasonic Absorbtion and Velocity Measurements. *J. Colloid Interface Sci.* **1989**, *132* (1), 145–160.
(23) Holmes, A. K.; Challis, R. E.; Wedlock, D. J. A Wide-Bandwidth

ation coefficient α_s has been calculated using the following expression for the single scattering losses:[1]

$$\alpha_s = \frac{\omega^4 a^3 \varphi}{2v_0^4}\left[\frac{1}{3}\left(\frac{\beta_0 - \beta_p}{\beta_0}\right)^2 + \left(\frac{\varrho_0 - \varrho_p}{2\varrho_p + \varrho_0}\right)^2\right] \quad (5.1)$$

where β_0 and β_p are the compressibilities of the liquid and particle. The particle compressibility is assumed here to be much smaller than the liquid compressibility.

The viscous attenuation coefficient has been calculated using expressions 2.5 and 2.19. The particle size is 5 μm and the density contrast is 3 for both mechanisms. There is no scattering attenuation compared with the viscous one for the smaller particles at frequencies below 100 MHz.

It is seen that scattering losses become comparable with viscous losses in the range of the high-frequency asymptote for the viscous losses. The frequency of the long-wave requirement is about 15 MHz for particles of size 5 μm. It is seen that there is no scattering attenuation at all in the low-frequency range where the long-wave requirement is valid.

LA951085Y